Ka-band Coaxial Horn Filtenna for Enhanced Electromagnetic Compatibility on Spacecraft

Matteo Oldoni
R&D Microwave Lab.
SIAE Microelettronica
Milano, Italy
matteo.oldoni@siaemic.com

Steven Caicedo Mejllones
Electronics and Information Dept.
Politecnico di Milano
Milano, Italy
stevenkleber.caicedo@polimi.it

Steven Caicedo Mejillones is also with
R&D Microwave Lab.
SIAE Microelettronica
Milano, Italy
steven.caicedo@siaemic.com

Stefano Moscato
R&D Microwave Lab.
SIAE Microelettronica
Milano, Italy
stefano.moscato@siaemic.com

Andrea Giannini
Satellites & Mission Business Unit
OHB Italia
Milano, Italy
andrea.giannini@ohb-italia.it

***Abstract*—Coexistence of wireless data links and radio sensing instruments onboard scientific satellites renews challenges concerning electromagnetic compatibility. Integration of filtering functions into the downlink antenna offers a space-effective way to improve isolation by suppressing out-of-band emissions. The present manuscript describes a filtenna design based on insertion of radial stubs into a coaxial horn and provides simulated results validating the principle.**

Keywords—electromagnetic compatibility, coaxial waveguide, circular horn, filtenna.

I. Introduction

The rising commercial interest towards the miniaturization of electronic components is leading a profound revolution in the space industry, mainly driven by mass and volumes minimization on spacecraft and launchers to meet a design-to-cost approach. The satellite-based Earth Observation market travels by contrast on a parallel track, pushing in the direction of improved performance of sensing instruments, which leads to high data resolution and therefore to large information throughput on the Space-to-Earth link. This inevitably raises concerns about coexistence of sensitive instruments and powerful transmitters. In this context, electromagnetic compatibility (EMC) becomes a fundamental engineering aspect in space flight programs.

A track record of failures or anomalies detected in historical NASA missions and proven to be the consequence of unmitigated electromagnetic interference is documented in [1]. Recently, the European Space Agency (ESA) have undergone serious challenges in ensuring EMC on MetOp, a meteorological space program in cooperation with EUMETSAT [2]. The spacecraft embarks a variety of very sensitive receivers, which demanded an extreme reduction of external in-band radiated emissions down to -28 dBμV/m.

The European Cooperation for Space Standardization (ECSS) has contributed in the years to develop standards and handbooks to pursue space systems EMC [3, 4, 5]. According to ECSS guidelines, a good design practice is based first on EMC assessment to be then verified during the Flight Acceptance Review (FAR), i.e. the last step before launch. In this frame, the following aspects shall be stressed:

- Friis transmission is used for early assessment of radiated coupling between two units provided that far-field conditions are met. However, this approach is not applicable if units are located close-by.
- Full-wave solvers can be exploited only in case antenna radiation patterns are available, if the unit is procured from an external supplier. In this case, antenna models or simulated radiation patterns are generally not disclosed by the manufacturer. In addition, the out-of-band antenna pattern is generally neither simulated nor measured.
- The cost burden and the long lead-times needed to access certified EMC testing facilities might not be affordable for all space programs or for medium-small enterprises.

The aim of this paper is to present an innovative concept that may help to re-think the classical EMC approach on space systems. The proposed solution foresees the embedding of a stop-band filter into a transmitting antenna (filtenna) to mitigate its spurious emissions against a susceptible "victim" unit. The presented filtenna is designed according to Table 1 to enable transmission to ground of scientific data in the portion of Ka-band reserved for Earth Exploration and Space Research Satellite service [6].

TABLE 1 – KA-BAND FILTENNA DESIGN TARGETS

Passband	25.5–27 GHz	RL>15dB, Max gain>19dBi, Axial Ratio>3.5dB within HPBW
Stopband	35.5–36 GHz	Gain suppression >30dB in all directions (with respect to passband)

The identified victim is a hypothetical radiometer for improved sensing of snow and ice thickness [7] whose operating frequency corresponds to the filtenna stopband. The proposed case demonstrates a solution for the support of the new Earth-Observation programs which raised interest in this technology, e.g the Copernicus Polar Ice and Snow Topography Altimeter (CRISTAL) ESA mission [8].

Based on the requirements, a circular horn is the chosen antenna, as its flare can accommodate an inline filter topology. Axial symmetry must be guaranteed throughout the whole structure, in order to preserve the input polarization (determined by the two input TE_{11} modes) and avoid excitation of modes with azimuthal index (N_φ) other than 1 along the progressively larger horn. The required stopband is achieved by extracted-pole transmission zeros (TXZs): they fit the inline form (no cross-couplings) and guarantee independent placement of each TXZ. Radial stubs fulfill all such constraints and their principle is discussed in Sect. II. Sect. III details the design workflow and Sect. IV reports the simulated filtenna and its performance.

This work was supported by the European Union's Horizon 2020 Research Program 5G STEP FWD under Grant 722429.

II. Radial Stubs for Filtenna Design

Radial waveguides work by propagation of cylindrical waves from the central axis. By making these guides "thin", the fields can be considered constant along the longitude z (k_z=0). The general scalar potential of cylindrical modes $C(\rho,\varphi,z)$ exhibits outward propagation along the radius ρ according to the Hankel function $H_2^{(N_\varphi)}(x)= J^{(N_\varphi)}(x)-jY^{(N_\varphi)}(x)$:

$$C(\rho,\varphi,z)=H^{(N_\varphi)}(k_\rho\rho)\cdot\sin(N_\varphi\varphi)\cdot e^{jzk_z} \quad \text{with} \quad k_\rho^2=\omega^2\mu\varepsilon-k_z^2$$

The radial phase is shown in Fig. 1, which is asymptotically linear: $-k_\rho\rho+N\varphi\pi/2-\pi/4$ with $\lambda_\rho=2\pi/k_\rho$ as radial wavelength.

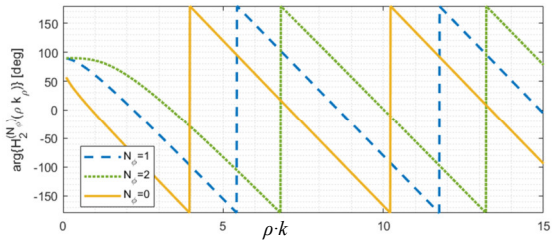

Figure 1. Radial phase of cylindrical waves

A thin short-circuited radial stub [9] resonates when the radial phase at its radius $\rho=R_{Out}$ is $N\cdot180°$, coinciding with the TM_{1N0} mode of a cylindrical cavity and also with the TM_{1N} cutoff frequency of a circular waveguide. For instance, N=2 requires $\omega(\mu\varepsilon)^{1/2}R_{Out}$=7, which resonates an R_{Out}=13.4 mm-stub at 24.9 GHz. When the same radial stub is excited by the TE_{11} of a circular waveguide, the TXZ is slightly affected: it occurs at 24.5 GHz when the feed waveguide has Ø=$2\cdot R_{In}$=7.795 mm and at 27.46 GHz for Ø=12.95 mm. Shrinking the stub radius increases the TXZ frequency, but a bound remains (Fig. 2): the TXZ becomes progressively narrower in bandwidth and then, beyond the feed's TM_{11} cutoff, it gradually disappears.

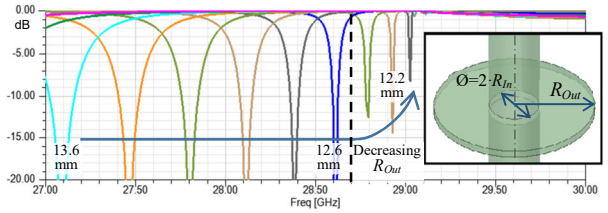

Figure 2. $|S_{21}|$ through waveguide (Ø 12.75 mm, cutoff TM_{11} 28.7 GHz) with radial stub (height 2 mm, R_{Out} decreased from 13.6 to 11.8 mm in 0.2 mm steps)

This phenomenon severely limits the application of the principle to a horn filtenna, as the flare of a standard hollow horn lowers the TM_{11} cutoff frequency along its body. As countermeasure, a coaxial metal core can be introduced into the horn: the thinner the open annular ring, the further up the TM_{11} and the further down the TE_{11} cutoffs, according to the corresponding transcendental equation [10] (Fig. 3, left).

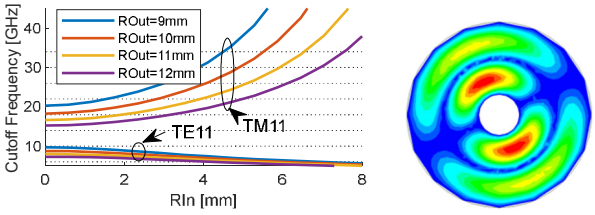

Figure 3. Left: TE_{11} and TM_{11} cutoff frequency for various inner (R_{In}) and outer radii (R_{Out}); right: field distribution at N=2 coaxial stub resonance

In a coaxial waveguide, radial stubs must be designed by using Fig. 1 so that the radial phases at the inner (R_{In}) and at outer radii (R_{Out}) are $N\cdot180°$ apart at the transmission zero frequency, as visible in Fig. 3 (right).

III. Design Principle

Coaxial radial stubs provide a simple yet powerful way to implement extracted poles. The 30 dB stopband is chosen as 600 MHz wide (100 MHz beyond the target). A 2nd order normalized all-pole filter with 30 dB of RL has been synthesized; then S_{11} and S_{21} were swapped to get the stopband behavior: the RL curve becomes the IL one, with two TXZs (Fig. 4). The denormalized synthesized circuit is found to require two stubs with 250 MHz of 15 dB-stopband each. The synthesis method [11] assumes constant coupling over frequency but the two stubs will be placed 270° apart, thus introducing slight RL degradation in the passband.

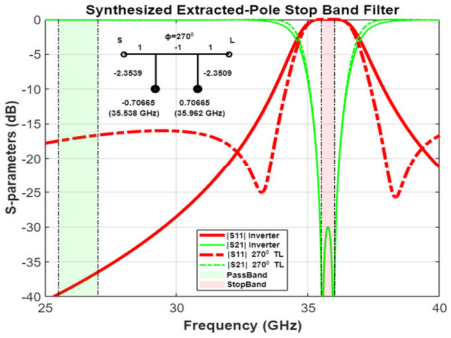

Figure 4: Topology of the required stopband filter and responses with ideal coupling ("inverter" curves) and a real 270° transmission line ("TL" curves)

In order to fit the prototype, two conditions are envisioned:

- the TM_{11} cutoff frequency must remain "high" in order to allow the required stopband width of each stub, while retaining an annular thickness sufficient to avoid high field concentration to contain losses;
- the TE_{11} impedance should remain approximately constant between the two stubs.

The proposed design flow is therefore as follows:

1. design a standard hollow circular horn to provide the required gain in the passband;
2. insert a coaxial metal core such that: the input section gradually transitions between circular and coaxial TE_{11} mode; the middle section must create a suitable annular opening to fulfill the two previous conditions; the terminal part must narrow down up to the horn's mouth, for correct aperture illumination and same passband gain;
3. insert the coaxial stubs in the middle section, dimensioning each stub according to their resonance frequency and on the filter prototype.

For the use case at hand, step 1 yields a horn with aperture diameter of 50 mm and length of 65 mm for a 20 dBi gain, fed by a 7.795 mm-Ø circular waveguide. Step 2 instead requires introducing and optimizing the coaxial core. The obtained TE_{11} impedance and TM_{11} cutoff can be evaluated to identify a suitable region for the two stubs, highlighted in red in Fig. 5. In step 3 finally the two stubs have been dimensioned for the required resonance and properly spaced at about 270° from each other. This preliminary design is finalized as described in Sect. IV.

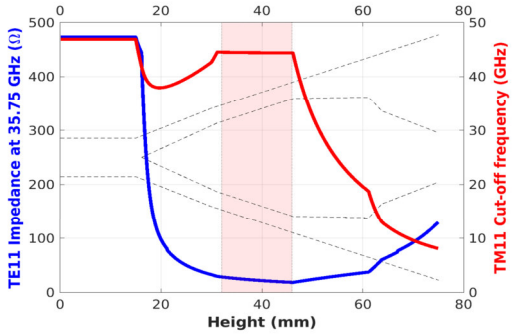

Figure 5: TE_{11} impedance and TM_{11} cutoff along the coaxial horn

IV. Design and Simulation Results

The preliminary theoretical design of the proposed filtenna results in a manufacturable structure, optimized through a full-wave simulator. The inner coaxial metal core inside the standard horn has been adjusted in its radial profile and is supported by two 4 mm-thick Teflon rings.

The design is detailed in Fig. 6; it has been simulated by Ansys HFSS (FEM method with radiation boundaries): fig. 7 (top) shows input matching and normalized maximum realized gain versus frequency. The matching in the passband is better than 18 dB (>15 dB required). The realized gain curve is normalized to the maximum gain at 26.25 GHz and shows a constant behaviour (within ±0.2 dB) in the passband and a 30.5 dB drop of radiated power within the designated stop-band (>30 dB required). Fig. 7 (bottom) shows the far-field characteristic of the whole design, summarized as the superposition of the radiation patterns of the LHC polarization and its cross-polarization counterpart at both 26.25 and 35.75 GHz. At 26.25 GHz the maximum gain is 19.6 dBi (>19 dBi required), while the HPBW is 13° (±6.5°) and within this angle the axial ratio is lower than the required 3.5 dB. The gain suppression between the 35.75 GHz stopband curve and the 26.25 GHz passband one is averagely more than 30 dB (neglecting radiation nulls).

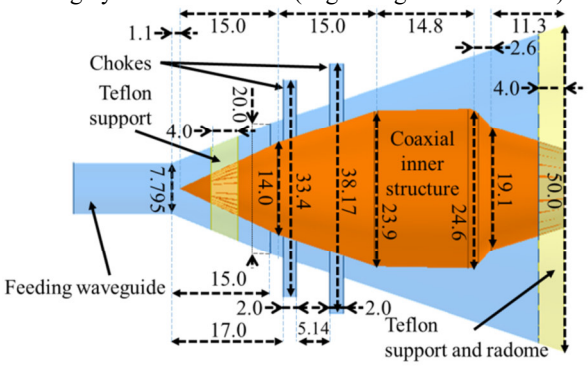

Figure 6. Lateral view of the proposed coaxial horn filtenna. Outer profile (blue) is piecewise linear and the total length is 60 mm. Inner profile (orange) is piecewise linear with 2 mm-radius fillet.

Concerning manufacturability, the outer horn can be assembled with a stack-up of laser cut metal layers, a technology currently exploited for horn arrays up to W-band. Alternatively, it can be manufactured as 3 thick lathed sections. The coaxial core can also take advantage of CNC lathing thanks to its full axial symmetry whereas, for weight reduction, the core can also be made hollow. The dielectric Teflon rings can similarly be manufactured by lathing and inserted onto the coaxial structure before it being placed into the hollow horn. The outermost Teflon ring also works as radome to avoid debris to enter the antenna; for its exposure to space radiation, specific surface treatments are needed.

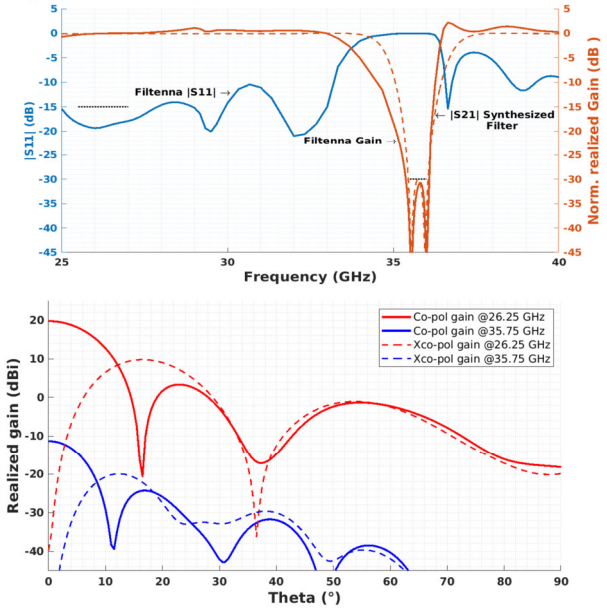

Figure 7. Top: S_{11} and normalizd realized gain versus frequency of the coaxial horn filtenna (solid lines) along with |S21| of the synthesized filter (dashed). Bottom: radiation pattern cuts in passband and stopband centers.

V. Conclusions

This work proposes a theoretical approach and a realistic design of a medium gain coaxial horn filtenna which allows correct far-field behavior within its operational bandwidth and total reflection across the 500 MHz selected span. This approach eases the EMC design on spacecraft by allowing >30 dB out-of-band radiation pattern suppression (rejection) to be directly embedded into the antenna sub-system.

References

[1] R. D. Leach and M. B. Alexander, "Electronic Systems Failures and Anomalies Attributed to EM Interference," Marshall Space Flight Center, Alabama 35812, NASA Reference Publ. 1374, July 1995.

[2] A. Ciccolella, F. Marliani, "EMC in Space Systems: Current Practices and Future Needs - The ESA Perspective", The Radio Science Bulletin no. 328, March 2009.

[3] ECSS-E-ST-20C, *Electrical and Electronic Engineering*, European Cooperation for Space Standardization, October 2019.

[4] ECSS-E-ST-20-07C, *Electromagnetic Compatibility*, European Cooperation for Space Standardization, February 2012.

[5] ECSS-E-HB-20-07A, *Electromagnetic Compatibility Handbook*, European Cooperation for Space Standardization, September 2012.

[6] ECSS-E-ST-50-05C Rev. 2, *Radio frequency and modulation*, European Cooperation for Space Standardization, October 2011.

[7] L. Gourdeau et al., "Altimetry in a Regional Tropical Sea [Space Agencies]," IEEE Geoscience and Remote Sensing Magazine, vol. 5, no. 3, pp. 44-52, September 2017.

[8] Kern, M., *et al.*, "The Copernicus Polar Ice and Snow Topography Altimeter (CRISTAL) high-priority candidate mission", The Cryosphere, no. 14, 2235–2251, 2020.

[9] J. Bornemann and S. Y. Yu, "Novel designs of polarization-preserving circular waveguide filters," International Journal of Microwave and Wireless Tech., vol. 2, no. 6, pp. 531–536, 2010.

[10] D. Pozar, "Microwave Engineering", ISBN 978-0-470-63155-3, John Wiley & Sons, Fourth Edition, 2012

[11] S. Caicedo Mejillones, *et al.*, "Accurate Synthesis of Extracted-Pole Filters by Topology Transformations," in IEEE Microwave and Wireless Components Letters, vol. 31, no. 1, pp. 13-16, Jan. 2021